Optical transitions in strained InAsSb/GaInSb interband QC lasers

Ligong Yang (杨立功), Peifu Gu (顾培夫), and Xiaoyun Qin (秦小芸)

Department of Optical Engineering, Zhejiang University, Hangzhou 310027

Received October 14, 2003

In this paper a detailed simulation and theoretical analysis based on model-solid theory and the $\vec{k}\cdot\vec{p}$ method are presented to investigate the dependence of the band structure on the strain deformation in a novel type-II quantum well (QW) heterostructure $InAs_{1-y}Sb_y/Ga_xIn_{1-x}Sb$ under the uniaxial approximation, and subsequently the optical transition and the gain in the interband cascade lasers containing it have been evaluated with unchanged injection current densities. The simulation results show that the strain effect on the transition in this heterostructure will not behave as a simple monotonic trend with the lattice mismatch of $InAs_{1-y}Sb_y/Ga_xIn_{1-x}Sb$ interface, but as a function of the complex strain chain including the whole active region. It is important to the subsequent device design and optimization.

OCIS codes: 140.5960, 140.3070, 140.3380, 160.6000.

So far many efforts have been made to improve the operation of the conventional interband quantum cascade (QC) lasers from the design of laser configuration to the devices fabrication[1−3]. From the view point of lattice-match, the lattice constant of $InAs_{1-y}Sb_y$ can be more flexible to be adjusted above or below the lattice constant of $Ga_xIn_{1-x}Sb$ in order that the band lineup can be more artificially tailored and the emission wavelength from this novel type-II quantum well (QW) heterostructure can be more adjustable. However, related reports about this configuration have not appeared as our knowledge, although even recently a compressively strained InAsSb/InAs multiple quantum-well (MQW) laser has been grown and tested[4]. Therefore it is worthy of studying this novel laser configuration and investigating their optical transition properties with strain. Note that here we generally assume the thickness given in this paper is below the critical value, which can be determined from the energy balance associated with the formation of a dislocation and plastic relaxation[5], to simplify the analysis model and implicate the physical trend from the analysis results.

To obtain an accurate strain alignment and band offsets, the model solid theory[6] combined with local-density-functional pseudopotential formalism is adopted to correctly evaluate the strain alignment and band offsets in these MQWs. We restrict our case within strained wells grown along the (001)-oriented (z-axis) direction, and hence the components of the stain tensor $\overline{\overline{e}}$ in every layer can be obtained exactly. Then the effects of the hydrostatic and shear deformation which interact with the conduction and the valence band can be evaluated.

The MQWs configuration of which we calculated the strain tensors is AlSb(20 nm)/$InAs_{1-y}Sb_y$(2 nm)/$Ga_xIn_{1-x}Sb$(3 nm)/AlSb(1.6 nm)/GaSb(5.8 nm)/AlSb (20 nm). The bold-noted layers denote the most key layers where the optical transition occurs. Here we assume the thickness of the AlSb to be large enough so as to neglect the effects between the neighboring stages. Sequentially the light hole band E_{V1}, the heavy hole band E_{V2}, the spin-orbit split-off band E_{V3}, and the conduction band E_C of $InAs_{1-y}Sb_y/Ga_xIn_{1-x}Sb$ layers with the constant thickness are calculated and shown in Figs. 1 and 2. In these figures one can find the bandgaps of these strained layers are overlapped when the values of x and y are set within certain regions. It shows that there probably exists strain-induced semimetal-semiconductor transition in these broken-gap QWs. The gap positions and magnitudes, however, also depend on the spin orientation of 2D hybridized electrons/holes and the detailed QWs structure. Moreover, the gap positions in energy and $k_{//}$ space are different in different direction of the in-plane $k_{//}$[7]. Hence the overlapped gap predicted by model-solid theory cannot strongly support this phase transition in $InAs_{1-y}Sb_y/Ga_xIn_{1-x}Sb$ QWs. In addition, we believe that this phenomenon also partially results from the neglect of the critical thickness constraint and should be properly determined by experiments. Thus in the subsequent analysis and simulation the gap position will be constrained in the normal-band-lineup region to circumvent this problem. We also estimated the band offset between $InAs_{1-y}Sb_y$ and $Ga_xIn_{1-x}Sb$. The estimation showed that this configuration could form the broken gap band edge alignments when $y \leq 0.4$ and $0.6 \leq x \leq 0.9$ under strain effects. Practically $Ga_{0.7}In_{0.3}Sb$ and $InAs_{0.9}Sb_{0.1}$ are the most popular semiconductor compounds used in semiconductor lasers, and here we consider the situations that the gallium composition x is near 0.7 and the antimony composition y is about 0.2.

We then employ the $\vec{k}\cdot\vec{p}$ method with the envelope-function approach to investigate the band structures. The electrical field across the device is neglected because the variation of electrical field has not a large impact on optical gain comparing with the case of zero electrical field[8], and the conduction-valence decoupling approximation is adopted for its good performance and simplicity[9,10]. According to the theory of Luttinger-Kohn[11] and Bir-Pikus[12] the valence band structure of a strained bulk semiconductor, which includes the coupling of spin-orbit splitting and other hole bands under compressively/tensilely strained or unstrained conditions, can be characterized by a 6×6 Hamiltonian under axial approximation[13]. All the parameters used in our model

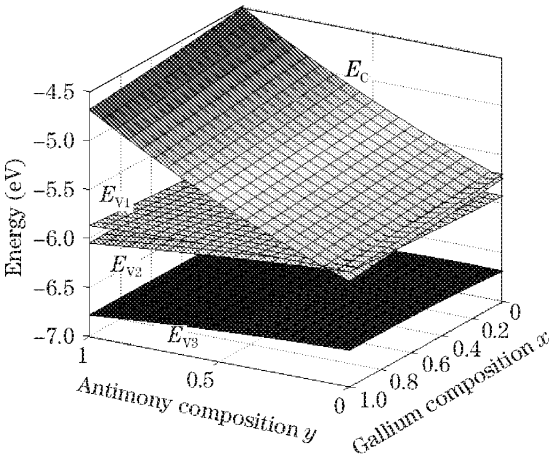

Fig. 1. Band edges at $\mathbf{k}_{//} = 0$ of the bottom conduction band E_C, the heavy hole band E_{V1}, the light hole band E_{V2} and the spin-orbit split-off band E_{V3} in strained $Ga_xIn_{1-x}Sb$ layer. Its thickness is 3 nm.

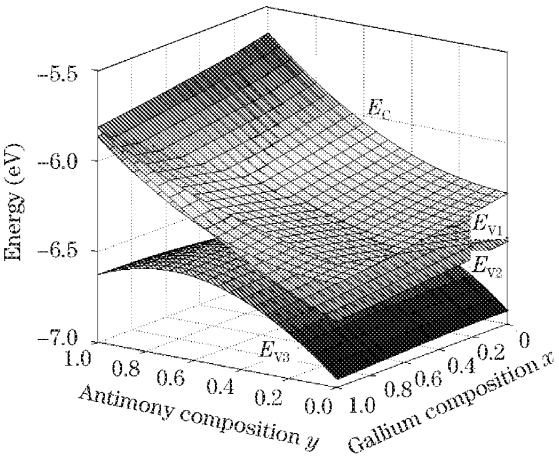

Fig. 2. Band edges at $\mathbf{k}_{//} = 0$ of the bottom conduction band E_C, the heavy hole band E_{V1}, the light hole band E_{V2} and the spin-orbit split-off band E_{V3} in strained $InAs_{1-y}Sb_y$ layer. Its thickness is 2 nm.

and calculation have been listed in Ref. [7]. In this model we ignored the temperature effects on the band structures and these material parameters. Figure 3 shows the wave functions of the first conduction subband C1 and the top three valence subbands HH1, HH2 and LH1 in one stage of the active region. It is obvious that in this structure the overlap region of the wave function C1 and the heavy hole subband wave function HH2 is dominant, but the mismatch is large. This will result in lower optical transition efficiency, which is much weaker than that of the conventional configuration if the intraband relaxation time is assumed to be same as that in the conventional configuration.

The valence band structure in the plane of the QWs under different strain conditions has been plotted in Fig. 4. Compared the first strained case where $x = 0.7$ and $y = 0.34$ so that the lattice constants of $InAs_{1-y}Sb_y/Ga_xIn_{1-x}Sb$ are matched, in the second strained case, the repulsion between HH1 subband and LH1 subband becomes stronger so that the valence

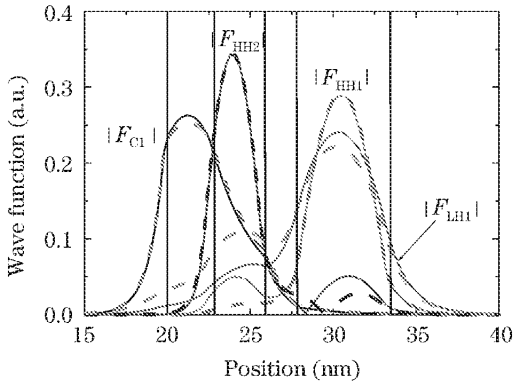

Fig. 3. The wave functions of the lowest conduction band and three topmost valence subbands at the zone center $\mathbf{k}_{//} = 0$ of one active region in the novel structure AlSb(20 nm)/$InAs_{1-y}Sb_y$(2.6 nm)/ $Ga_{0.7}In_{0.3}Sb$(3.6 nm)/AlSb(1.7 nm)/GaSb(5.6 nm)/AlSb(20 nm): $y = 0.3$ (dashed line) and $y = 0.1$ (solid line). The black perpendicular lines in this figure are denoted for the interface position in one active region.

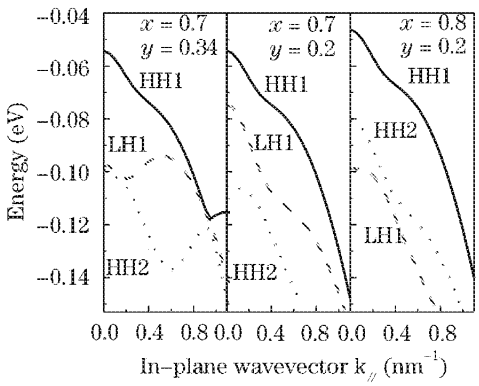

Fig. 4. The three top valence-subband dispersion curves for three combination cases of different x and y.

band mixing effect is reduced. Evidently it will affect the carrier relaxation and distribution in the valence subbands. Moreover, the simulation implies that even the lattice constants between the broken gap heterostructure are matched and the thickness is unchanged, the band structures in these cases are also definitely different because the strain existing at the other interfaces in the active region has to be included. This is an important character of interband QC lasers and can be confirmed by our third strained case, $x = 0.8$, $y = 0.2$, where the mismatch of the lattice constants between the broken gap heterostructure is less than 0.3% and the thickness of every QW is same as those in previous cases.

In practice, an interband QC laser consists of tens of stages described above. Generally, increasing the number of stages serves mainly to increase the mode occupation factor and enhance the quantum efficiency, and does not significantly change $g(\hbar\omega)$, the gain in one stage of the active region. Thus we simulate only the optical gain of one stage and it can be presented by assuming a Lorentzian line-shape function[10]. Within the simulation, we set $\Gamma = 10$ meV, a parameter that describes the line broadening factor from the carrier collision effect.

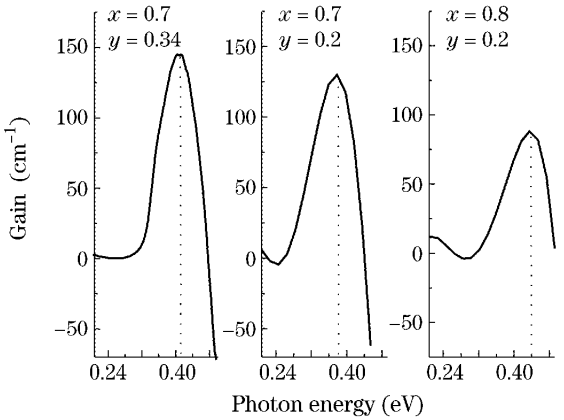

Fig. 5. The TE modes gain spectra of the novel configuration with different combinations of the composition x and y. The injection current density $n = 0.8 \times 10^{18}$ cm^{-3}. The dotted lines in the figure are guides to the eye.

It is obvious that the compressed relaxation efficiency and the mismatched wave functions in the active region affect the optical transition strength within the conduction-valence bands of the BG heterostructure, and hence the optical gain magnitude is determined.

In conclusion, we have theoretically investigated the band structure of a novel type-II QW structure, $InAs_{1-y}Sb_y/Ga_xIn_{1-x}Sb$, and the optical transition characters of the interband QC lasers embedding them under different strain conditions based on a simple model. The results show that in certain material component regions the lowest conduction subband and the top valence subband are overlapped and seem to exist a strain induced semimetal-semiconductor transition. However, further cautiously theoretical and experimental investigation should be performed to verify this conclusion. Additionally, the simulation analysis proves that the optical gain in the interband QC lasers embedding this broken gap structure is affected by the whole strain chain of the active region so that the optimization of the whole active region to this novel structure is more crucial, and these can be applied and compared in further research work.

L. Yang's e-mail address is yanglig@zju.edu.cn.

References

1. C. L. Felix, W. Bewley, I. Vurgaftman, J. R. Meyer, D. Zhang, C.-H. Lin, R. Q. Yang, and S. S. Pei, IEEE Photon. Technol. Lett. **9,** 1433 (1997).
2. I. Vurgaftman, J. R. Meyer, and L. R. Ram-Mohan, IEEE Photon. Technol. Lett. **9,** 170 (1997).
3. R. Q. Yang, J. L. Bradshaw, J. D. Bruno, J. T. Pham, D. E. Wortman, and R. L. Tober, Appl. Phys. Lett. **81,** 397 (2002).
4. B. Lane, D. Wu, A. Rybaltowski, H. Yi, J. Diaz, and M. Razeghi, Appl. Phys. Lett. **70,** 443 (1997).
5. E. P. O'Reilly and A. R. Adams, IEEE J. Quantum Electron. **30,** 366 (1994).
6. C. G. V. Walle, Phys. Rev. B **39,** 1871 (1989).
7. L. W. Wang, S. H. Wei, T. Mattila, and A. Zunger, Phys. Rev. B **60,** 5590 (1999).
8. Y. M. Mu and R. Q. Yang, in *Proceedings of Lasers and Electro-Optics Society Annual Meeting, LEOS'98* **2,** 317 (1998).
9. L. G. Yang and P. F. Gu, Proc. SPIE **5280,** (2003).
10. D. Ahn and S. Chuang, IEEE J. Quantum Electron. **24,** 2400 (1988).
11. J. M. Luttinger and W. Kohn, Phys. Rev. **97,** 869 (1955).
12. G. L. Bir and G. E. Pikus, *Symmetry and Strain-Induced Effects in Semiconductors* (Wiley, New York, 1974).
13. C. S. Chang and S. L. Chuang, IEEE J. Sel. Top. Quantum Electron. **1,** 218 (1995).